American Society of Hematology
2021 L Street NW, Suite 900,
Washington, DC 20036
Phone: 202-776-0544 | Fax 202-776-0545
editorial@hematology.org

Single cell analysis reveals immune dysfunction from the earliest stages of CLL that can be reversed by ibrutinib

Tracking no: BLD-2021-013926R2

Noelia Purroy Zuriguel (Dana-Farber Cancer Institute; Harvard Medical School, United States) Yuzhou Tong (Dana-Farber Cancer Institute; Harvard Medical School, United States) Camilla Lemvigh (Technical University of Denmark, Denmark) Nicoletta Cieri (Dana-Farber Cancer Institute, United States) Shuqiang Li (Broad Institute, United States) Erin Parry (Dana-Farber Cancer Institute, United States) Wandi Zhang (Dana-Farber Cancer Institute, United States) Laura Rassenti (University of California, San Diego, United States) Thomas Kipps (Moores Cancer Center, University of California, United States) Susan Slager (Mayo Clinic, United States) Neil Kay (Mayo Clinic, United States) Connie Lesnick (Mayo Clinic,) Tait Shanafelt (Stanford University School of Medicine, United States) Paolo Ghia (Università Vita-Salute San Raffaele, Italy) Lydia Scarfò (Laboratory of B cell Neoplasia, Division of Experimental Oncology, Istituto Scientifico San Raffaele, Italy) Kenneth Livak (Dana-Farber Cancer Institute, United States) Peter Kharchenko (Harvard Medical School, United States) Donna Neuberg (Dana-Farber Cancer Institute, United States) Lars Ronn Olsen (Technical University of Denmark, Denmark) Jean Fan (Johns Hopkins University, United States) Satyen Gohil (University College London, United Kingdom) Catherine Wu (Dana-Farber Cancer Institute; Harvard Medical School, United States)

Abstract:

Conflict of interest: COI declared - see note

COI notes: N.P. is currently an employee of AstraZeneca; CJW holds equity in BioNTech, Inc.; and receives research funding from Pharmacyclics; SHG has received speaker fees from Janssen UK, travel and honoraria from Abbvie, and undertakes research consultancy for Novalgen Limited. P.G. received honoraria from AbbVie, AstraZeneca, ArQule(MSD, BeiGene, Celgene/Juno/BMS, Janssen, Loxo/Lilly, Roche and research funding from AbbVie, AstraZeneca, Janssen, Sunesis. P.V.K serves on the Scientific Advisory Board to Celsius Therapeutics Inc. and Biomage Inc. N.E.K. Advisory Board for: Abbvie, Astra Zeneca, Behring, Cytomx Therapy, Dava Oncology, Janssen, Juno Theraputics, Oncotracker, Pharmacyclics and Targeted Oncology. DSMC (Data Safety Monitoring Committee) for: Agios Pharm, AstraZeneca, BMS -Celgene, Cytomx Therapeutics, Janssen, Morpho-sys, Rigel. Research funding from: Abbvie, Acerta Pharma, Bristol Meyer Squib, Celgene, Genentech, MEI Pharma, Pharmacyclics, Sunesis, TG Therapeutics, Tolero Pharmaceuticals. L.S. received honoraria from AbbVie, AstraZeneca, Janssen and travel funding from Janssen. T.D.S. received research support to institution from Genentech, Phamacyclics.

Preprint server: No;

Author contributions and disclosures: N.P., J.F., S.H.G. and C.J.W. designed and conceived the study; N.P., L.Z.R., T.J.K., S.L.S., N.E.K., C.L., T.D.S., P.G., and L.S. collected samples and clinical annotations; S.L. generated the single cell RNAseq libraries and processed the raw sequencing data; N.P., Y.E.T., C.K.L., N.C., E.M.P., D.S.N., J.F., and S.G. analyzed and interpreted data; J.F., S.G. and C.J.W. supervised the project; N.P., Y.T., S.G., and C.J.W. wrote the paper with assistance from all other authors.

Non-author contributions and disclosures: No;

Agreement to Share Publication-Related Data and Data Sharing Statement: We will deposit all single cell data into a public repository (dbGAP). Questions from readers regarding methods and protocols will be answered by email to the corresponding author. The dbGAP number for this study is Phs002705.v1.

Clinical trial registration information (if any):

Title

Single cell analysis reveals immune dysfunction from the earliest stages of CLL that can be reversed by ibrutinib

Authors

Noelia Purroy[1,2,3]*, Yuzhou Evelyn Tong[2,3,14]*, Camilla K. Lemvigh[1,4]*, Nicoletta Cieri[1,2,3], Shuqiang Li[3,5], Erin M. Parry[1,2,3], Wandi Zhang[1], Laura Z. Rassenti[6], Thomas J. Kipps[6], Susan L. Slager[7], Neil E. Kay[8], Connie Lesnick[8], Tait D. Shanafelt[9], Paolo Ghia[10], Lydia Scarfò[10], Kenneth J Livak[1,5], Peter V. Kharchenko[11], Donna S Neuberg[12], Lars Rønn Olsen[4], Jean Fan[16], Satyen H. Gohil[1,2,3,15] and Catherine J. Wu, MD[1,2,3,13]†

Affiliations

[1]Department of Medical Oncology, Dana Farber Cancer Institute, Boston, MA; [2]Harvard Medical School, Boston, MA, USA; [3]Broad Institute, Cambridge, MA, USA; [4]Department of Health Technology, Technical University of Denmark, Kongens Lyngby, Denmark; [5]Translational Immunogenomics Lab, Dana Farber Cancer Institute, Boston, MA, USA;[6]Moores Cancer Center, University of California, San Diego, La Jolla, CA, USA; [7]Department of Health Sciences Research, Mayo Clinic, Rochester, MN, USA; [8]Department of Medicine, Mayo Clinic, Rochester, MN, USA; [9]Stanford University, Stanford, CA, USA; [10]Division of Experimental Oncology and Department of Onco-Hematology, Università Vita-Salute San Raffaele and Istituto di Ricovero e Cura a Carattere Scientifico (IRCCS) Ospedale San Raffaele, Milano, Italy;[11]Department of Biomedical Informatics, Harvard Medical School, Boston, MA, USA; [12]Department of Data Science, Dana-Farber Cancer Institute, Boston, MA, USA; [13]Division of

Hematology, Department of Medicine, Brigham and Women's Hospital, Boston, MA, USA. [14]Program in Health Sciences & Technology, Harvard Medical School & Massachusetts Institute of Technology, Boston, MA, USA; [15]Department of Academic Haematology, University College London, UK; [16]Department of Biomedical Engineering, Johns Hopkins University, Baltimore, MD, USA.

* denotes equal contribution

† corresponding author

Correspondence to: cwu@partners.org

Word count: 1385

Chronic lymphocytic leukemia (CLL) is characterized by a clonal expansion of mature $CD19^{+}CD5^{+}$ B cells, which are highly dependent on microenvironmental cues for their survival[1]. This common adult leukemia is preceded by a precursor phase termed monoclonal B-cell lymphocytosis (MBL)[2,3] that has been characterized as indistinguishable from CLL at the genetic, transcriptomic and epigenomic level[4-6]. However, how leukemia cells co-evolve with immune cells in their circulating microenvironment during the onset of MBL and upon progression to CLL remains incompletely characterized[7].

Recently, single cell transcriptome sequencing approaches (scRNA-seq) have transformed our ability to gain a comprehensive evaluation of the spectrum of immune cells within the tumor microenvironment and of their potential crosstalk with cancer cells[8-14]. Herein, we applied scRNA-seq to broadly characterize circulating immune cells co-existing with leukemic cells

during natural CLL progression. Although we acknowledge the critical role of bone marrow and lymph nodes microenvironment on CLL cells, the lack of feasibility for procuring serial specimens from these tissue compartments led us to focus our study on circulating immune cells. We therefore collected serial peripheral blood mononuclear cell (PBMC) samples from 3 individuals with high count MBL who did not progress to CLL after a median follow-up of 7.0 years and 7 patients with CLL, whose genetic characterization of $CD19^{+}CD5^{+}$ cells over time by whole-exome sequencing (WES), has been previously reported [15] (**Figure 1A**). For all patients, we processed paired samples: the first time point (T1) was collected at a median of 4.96 years (range: 2.44-5.46) from MBL diagnosis or 2.54 years (range: 0.5-4.2) from CLL diagnosis; while the second time point (T2) was collected at a median of 2.97 years (range: 2.01-2.99) from T1 for the MBL patients and 4.75 years (range: 1.3-10.6) for the CLL patients. T2 samples for CLL patients were collected at a median of 0.2 years (range: 0-5.9) before first treatment (**Suppl Table 1**).

Non-$CD19^{+}CD5^{+}$ cells were isolated by fluorescence-activated cell sorting and samples from each patient were processed on the same day to minimize batch effect. Cell suspensions were loaded on a GemCode Single-Cell Instrument (10x Genomics) and libraries were prepared as previously described[16] (**Suppl Methods**). Analysis was conducted using Seurat V4.0.0 selecting cells with gene count between 500 and 3,000 and less than 10% mitochondrial reads. Using the trimmed dataset, we isolated the non-tumor population and assigned immune cell types by performing multimodal reference mapping using a CITE-seq reference of 162,000 PBMCs measured with 228 antibodies[17]. B cells were excluded due to potential CLL contamination. After quality control, we obtained 67,333 single cell transcriptomes (median number of cells per

sample: 3711, range 491-6633 cells) (**Figure 1B, Suppl Table 1**). For each sample, we evaluated the potential for processing and batch artefacts between samples and cohorts, and we selected cohorts with similar 'cold-shock signature'[18] for comparison (**Suppl Figure 1A**). In total, we identified 16 clusters across 3 distinct lineages: T cells, NK cells and myeloid cells (**Figure 1B, top UMAP**). The distribution of immune cell types from MBL and CLL samples and across patients appeared to be balanced across the cell clusters (**Figure 1B, bottom UMAP; Suppl Figure 1B**). Analysis of the proportions of immune cell types, including various T cell subsets, between MBL and CLL samples revealed no differences, even across time points (T1 vs T2) (**Figure 1C-D**; **Suppl Table 2a**).

To confirm the absence of major differences in immune cell proportions between MBL and CLL, we performed scRNAseq on PBMCs collected from a separate cohort of 4 high count MBL patients that progressed to CLL (MBL-CLL1-4); the median time from MBL (T1) to CLL diagnosis was 2.68 years (range, 0.7 – 4.6) and from CLL diagnosis to T2 was 0.6 years (range, 0 – 1.8). We also evaluated 2 age-matched healthy donors (HDs, median number of cells per sample: 4400, range 2630-7596 cells) using the same approach described above (**Figure 2A, B**). Again, we observed an absence of major compositional or phenotypic changes in immune cell populations in the transition from MBL to CLL, while marked differences in the composition in immune cell types were evident in CLL compared to HDs. In particular, the proportion of $CD8^+$ T cells was higher in CLL compared to HD (33% vs 8%, p=0.037), with a corresponding decrease in $CD4^+$ T cells (**Figure 2C, left panel; Suppl Table 2b**). The $CD4^+$ and $CD8^+$ T cell subtypes that contributed to these differences were naïve, central memory (TCM) $CD4^+$ and terminal effector memory (TEM) $CD8^+$ cells (**Figure 2C, right panel**). A higher number of

differentially expressed genes (DESeq adjusted p-value <0.05 and |avg_log_2FC| >0.6) was observed between HD and MBL/CLL patients than between MBL to CLL at the time of progression (MBL-CLL 1 and 2, **Figure 2D; Suppl Table 3**). More differences in gene expression were seen in those paired samples where CLL was sampled at a time more distant from transition to CLL (MBL-CLL 3 and 4), suggesting further evolution of the immune response over time with CLL progression. Effector memory $CD8^+$ T cells, $CD56^{dim}$ NK cells consistently showed more differentially expressed genes in both MBL and CLL versus HDs (**Figure 2D right panel**), which we also observed when re-analyzing these data as a pseudo-bulk analysis of the same data (**Suppl Fig 2**). Comparable shifts in immune cell expression profiles were observed in the evaluation of independent MBL (MBL1-3, T1) versus CLL (CLL1-7, T2), but only minimal differences were observed in non-progressing MBL (**Figure 2E**). While we acknowledge that the low number of replicates (n=2) does not provide sufficient power to detect the biological variability among HDs and that individual-specific variations might confound the observed differences between HDs and MBL/CLL samples, we minimized this risk by selecting age-matched HDs and applied uniform processing to all samples.

To investigate which dysfunctional immune mechanisms may potentially impact CLL biology, we interrogated major molecular interactions between immune and normal B or CLL-B cells in HDs or patients, respectively, using CellPhoneDB v2.1.7 which predicts potential interactions between ligand–receptor pairs based on elevated expression in the corresponding cell-types[19]. In so doing, we observed an increased total number of potential interactions in subjects with MBL compared to HDs. This increase remained stable with progression to CLL and was evident across diverse immune cell types but most distinctly observed in monocytes (**Figure 2F, left heatmap**).

To examine the effects of B cell receptor (BCR) signaling inhibition with ibrutinib on the cellular interactions between immune and leukemia cells, we re-analyzed 4 additional scRNA-seq samples previously generated from PBMCs before and during ibrutinib treatment (cells collected 30-240 days after treatment) from two patients with CLL[20,21]. We again observed that the number of cellular interactions in pre-treatment CLL samples was higher across immune cell types and especially in monocytes in both patients. Consistently, the number of interactions decreased after ibrutinib treatment to levels similarly observed in HDs (**Figure 2F, right heatmaps**). Most of the interactions upregulated in MBL/CLL patients involved inhibitory signals of immune cell function proceeding from CLL cells across to various immune cell types such as: *BTLA/MIF-TNFRSF14 (HVEM*, observed in MBL-CLL1, 3 and 4), *CTLA4-CD86* (observed in MBL-CLL4)*,* and *LGALS9-HAVCR2 (TIM3,* observed in MBL-CLL1-4) (**Figure 2G, left panel and Suppl Fig 3)**. Notably, only a proportion of cancer cells express these inhibitory signals: *BTLA* (17.4%), *MIF* (41.6%), *LGALS9* (18.2%), and *CTLA4* (10.4%) (**Suppl Fig 4**). We observed that all these interactions were downregulated after ibrutinib treatment (**Figure 2G, right panels**).

Altogether, we observed that the composition and state of immune cells was markedly different between HDs and MBL patients, while no major additional transcriptional changes manifested during natural progression from MBL to CLL. These observations suggest that the key drivers of transcriptional immune dysfunction in CLL may be present early during the course of the disease and are in keeping with the early transcriptomic, genomic and epigenetic changes already present in MBL as well as the known increased risk of infections even at the earliest stages of the disease[22]. Among the features that distinguished immune and leukemia cells interactions in

patients with CLL were an increased number of cellular interactions compared to HDs, especially within myeloid cells, that predominantly involved multiple inhibitory immune signals, and which were no longer detected after ibrutinib treatment. Thus, although T cell deficits in CLL have been well investigated[23,24], the contribution of myeloid cells to inhibitory signals has been far less characterized and warrants further assessment.

ACKNOWLEDGEMENTS

We thank Jerome Ritz and the DFCI Pasquarello Tissue Bank in Hematologic Malignancies for prospective collection and processing of blood samples from healthy donors. This work was supported in part by the NCI (5P01CA081534-14, P01CA206978, R01CA216273, UG1CA233338). C.J.W. acknowledges support from the CLL Global Research Foundation. SHG was supported by a Kay Kendall Leukaemia Fund Fellowship. EMP acknowledges support from Research funding Doris Duke Charitable Foundation (Physician-Scientist Fellowship), Conquer Cancer (The ASCO Foundation) Young Investigator Award, Dana-Farber Flames FLAIR. J.F acknowledges support from the NIGMS under Award Number R35GM142889. PG acknowledges support from Associazione Italiana per la Ricerca sul Cancro – AIRC, Milano, Italy (Special Program on Metastatic Disease – 5 per mille #21198) and ERA NET TRANSCAN-2 Joint Transnational Call for Proposals: JTC 2016 (project #179 NOVEL), project code (MIS) 5041673. S.L. is supported by the NCI Research Specialist Award (R50CA251956).

AUTHORSHIP CONTRIBUTIONS

N.P., J.F., S.H.G. and C.J.W. designed and conceived the study; N.P., L.Z.R., T.J.K., S.L.S., N.E.K., C.L., T.D.S., P.G., and L.S. collected samples and clinical annotations; S.L. generated

the single cell RNAseq libraries and processed the raw sequencing data; N.P., Y.E.T., C.K.L., N.C., E.M.P., D.S.N., J.F., and S.G. analyzed and interpreted data; J.F., S.G. and C.J.W. supervised the project; N.P., Y.T., S.G., and C.J.W. wrote the paper with assistance from all other authors.

Disclosure of conflict of interest:

N.P. is currently an employee of AstraZeneca; CJW holds equity in BioNTech, Inc.; and receives research funding from Pharmacyclics; SHG has received speaker fees from Janssen UK, travel and honoraria from Abbvie, and undertakes research consultancy for Novalgen Limited. P.G. received honoraria from AbbVie, AstraZeneca, ArQule(MSD, BeiGene, Celgene/Juno/BMS, Janssen, Loxo/Lilly, Roche and research funding from AbbVie, AstraZeneca, Janssen, Sunesis. P.V.K serves on the Scientific Advisory Board to Celsius Therapeutics Inc. and Biomage Inc. N.E.K. Advisory Board for: Abbvie, Astra Zeneca, Behring, Cytomx Therapy, Dava Oncology, Janssen, Juno Theraputics, Oncotracker, Pharmacyclics and Targeted Oncology. DSMC (Data Safety Monitoring Committee) for: Agios Pharm, AstraZeneca, BMS –Celgene, Cytomx Therapeutics, Janssen, Morpho-sys, Rigel. Research funding from: Abbvie, Acerta Pharma, Bristol Meyer Squib, Celgene, Genentech, MEI Pharma, Pharmacyclics, Sunesis, TG Therapeutics, Tolero Pharmaceuticals. L.S. received honoraria from AbbVie, AstraZeneca, Janssen and travel funding from Janssen. T.D.S. received research support to institution from Genentech, Phamacyclics.

REFERENCES

1 Burger J. A. The CLL cell microenvironment. *Adv Exp Med Biol.* 2013;**792**, 25-45.

2 Dagklis A., Fazi, C., Scarfo, L., Apollonio, B. & Ghia, P. Monoclonal B lymphocytosis in the general population. *Leuk Lymphoma*. 2009**;50**, 490-492.

3 Rawstron A. C., Benett F.L., O'Connor S.J.M. *et al.* Monoclonal B-cell lymphocytosis and chronic lymphocytic leukemia. *N Engl J Med.* 2008;**359**, 575-583.

4 Puente X. S., Beà S., Valdés-Mas R., *et al.* Non-coding recurrent mutations in chronic lymphocytic leukaemia. *Nature*. 2015; **526**, 519-524.

5 Agathangelidis, A., Ljungström V., Scarfò L., *et al.* Highly similar genomic landscapes in monoclonal B-cell lymphocytosis and ultra-stable chronic lymphocytic leukemia with low frequency of driver mutations. *Haematologica*. 2018;**103**, 865-873.

6 Kretzmer H., Biran A., Purroy N., *et al*. Preneoplastic Alterations Define CLL DNA Methylome and Persist through Disease Progression and Therapy. *Blood Cancer Discov*. 2021;2(1):54-69.

7 Purroy N., Wu CJ. Coevolution of leukemia and host immune cells in Chronic Lymphocytic Leukemia. *Cold Spring Harb Perspect Med*. 2017;7(4):a026740.

8 Plass M., Solana J., Wolf F.A., *et al.* Cell type atlas and lineage tree of a whole complex animal by single-cell transcriptomics. *Science*, 2018; 360(6391):eaaq1723.

9 Villani A. C., Satija R., Reynolds G., *et al.* Single-cell RNA-seq reveals new types of human blood dendritic cells, monocytes, and progenitors. *Science,* 2017;356(6335):eaah4573.

10 Navin,N., Kendall J., Troge J., *et al.* Tumour evolution inferred by single-cell sequencing. *Nature*.2011;472(7341):90-94.

11 Patel A. P., Tirosh I., Trombetta J.J., *et al.* Single-cell RNA-seq highlights intratumoral heterogeneity in primary glioblastoma. *Science*. 2014;344(6190):1396-1401.

12 Tirosh I., Izar B., Prakadan S.M., *et al.* Dissecting the multicellular ecosystem of metastatic melanoma by single-cell RNA-seq. *Science*. 2016;352(6282):189-196.

13 Gohil S.H., Iorgulescu J.B., Braun D.A., Keskin D.B., Livak K.J. Applying high-dimensional single-cell technologies to the analysis of cancer immunotherapy. *Nat Rev Clin Oncol*. 2021 Apr;18(4):244-256.

14 Roerink S. F., Sasaki N., Lee-Six H., *et al.* Intra-tumour diversification in colorectal cancer at the single-cell level. *Nature*. 2018;556(7702):457-462.

15 Gruber M., Bozic I., Leshchiner I., *et al*. Growth dynamics in naturally progressing chronic lymphocytic leukemia. *Nature*. 2019;570(7762):474-479.

16 Zheng G. X., Terry J.M., Belgrader P., *et al.* Massively parallel digital transcriptional profiling of single cells. *Nat Commun*. 2017; **8:**14049.

17 Hao Y., Hao S., Andersen-Nissen E., *et al*. Integrated analysis of multimodal single-cell data. *Cell*. 2021;184(13):3573-3587.e29.

18 Massoni-Badosa R., Iacono G., Coutinho C. et al. Sampling time-dependent artifacts in single-cell genomics studies. *Genome Biol*. 2020;21(1):112

19 Efremova M., Vento-Tormo M., Teichmann S.A., Vento-Tormo R. CellPhoneDB: inferring cell–cell communication from combined expression of multi-subunit ligand–receptor complexes. *Nat Protoc*. 2020;15(4), 1484-1506.

20 Rendeiro A.F., Krausgruber T., Fortelny N., *et al.* Chromatin mapping and single-cell immune profiling define the temporal dynamics of ibrutinib in CLL. *Nat Commun*. 2020;11(1):577.

21 Gutierrez C., Al'Khafaji A.M., Brenner E., et al. Multifunctional barcoding with ClonMapper enables high-resolution study of clonal dynamics during tumor evolution and treatment. *Nature Cancer*. 2021; **2**:758–772.

22 Moreira J., Rabe K.G., Cerhan J.R., et al. Infectious complications among individuals with clinical monoclonal B-cell lymphocytosis (MBL): a cohort study of newly diagnosed cases compared to controls. *Leukemia*. 2013;27(1):136-41.

23 Ramsay A.G., Johnson A.J., Lee A.M., et al. Chronic lymphocytic leukemia T cells show impaired immunological synapse formation that can be reversed with an immunomodulating drug. *J Clin Invest.* 2008;118(7):2427-37.

24 Long M., Beckwith K., Do P., et al. Ibrutinib treatment improves T cell number and function in CLL patients. *J Clin Invest.* 2017;127(8):3052-3064.

FIGURE LEGENDS

Figure 1. scRNAseq analysis of immune cells from non-progressive MBL patients and CLL patients. (A) Peripheral blood mononuclear cells from 2 serial samples were collected for 3 MBL (red dots) and 7 CLL patients (purple dots). **(B)** Non-$CD19^{+}CD5^{+}$ cells were isolated by fluorescence-activated cell sorting. Uniform manifold approximation and projection (UMAP) visualization of all immune cells. Cells are colored by immune cell type (top) and CLL or MBL assignment (bottom). **(C)** Proportion of immune cell types per time point in MBL and CLL patients. (**D**) Proportion of T cell types per time point in MBL and CLL patients. Cell percentages were calculated after averaging cell numbers from all samples. Abbreviations: DC, Dendritic cell; pDC, Plasmacytoid dendritic cell; Mono, Monocyte; T, T-cell; NK, Natural killer cell; ILC, Innate lymphoid cells; gdT, Gamma-delta T cells; MAIT, Mucosal associated invariant T cells; TCM, Central memory T cells; TEM, Effector memory T cells; CTL, Cytotoxic T cells; Treg, Regulatory T cells.

Figure 2. scRNAseq analysis of immune cells from healthy donors and progressive disease from MBL to CLL. (A) scRNAseq was performed on PBMCs collected from 4 MBL patients (red dots) that progressed to CLL (purple dots), and from 2 healthy donors (blue dots). Symbol X indicates the time of diagnosis of CLL. **(B)** UMAP visualization of all immune cells colored by immune cell types (left) and by sample types (right). **(C)** Proportion of immune cell types (left) and T cell subtypes (right). **(D)** Number of significant differentially expressed genes for each cell type by performing comparison of paired samples within patients (left panel) or comparison between MBL samples or CLL samples versus healthy donors (right panel). Cells were

categorized based on lymphoid and myeloid cells. (**E**) Same analysis for significant differentially expressed genes was performed on 3 independent non-progressive MBL patients and 7 CLL patients (from **Figure 1**). **(F)** Heatmaps with the number of the significant ligand-receptor interactions for each cell type under different conditions using CellPhoneDB v2.1.7. Heatmap comparing the number of significant interactions between healthy donors and patient samples from either MBL stage or CLL stage (left). Heatmaps including samples before and after ibrutinib for two additional patients (right panels). Grey boxes indicate insufficient number of cells to perform interactome analysis. **(G)** Heatmaps representing the difference of p-values for each ligand-receptor pair regarding specific cell types (x-axis). Interactions that are enriched in patients (red) or enriched in healthy donors (blue) were calculated by subtracting $-\log_{10}$(p-value) in healthy donors from $-\log_{10}$(p-value) in patients (left panel). The same interactions that are either enriched (red) or depleted (blue) after ibrutinib (right panels) are calculated by subtracting $-\log_{10}$(p-value) in pre-ibrutinib from $-\log_{10}$(p-value) in post-ibrutinib. Abbreviations: HDs, Healthy donors; Pts, Patients; cell type abbreviations are the same as in **Figure 1**.

Figure 1

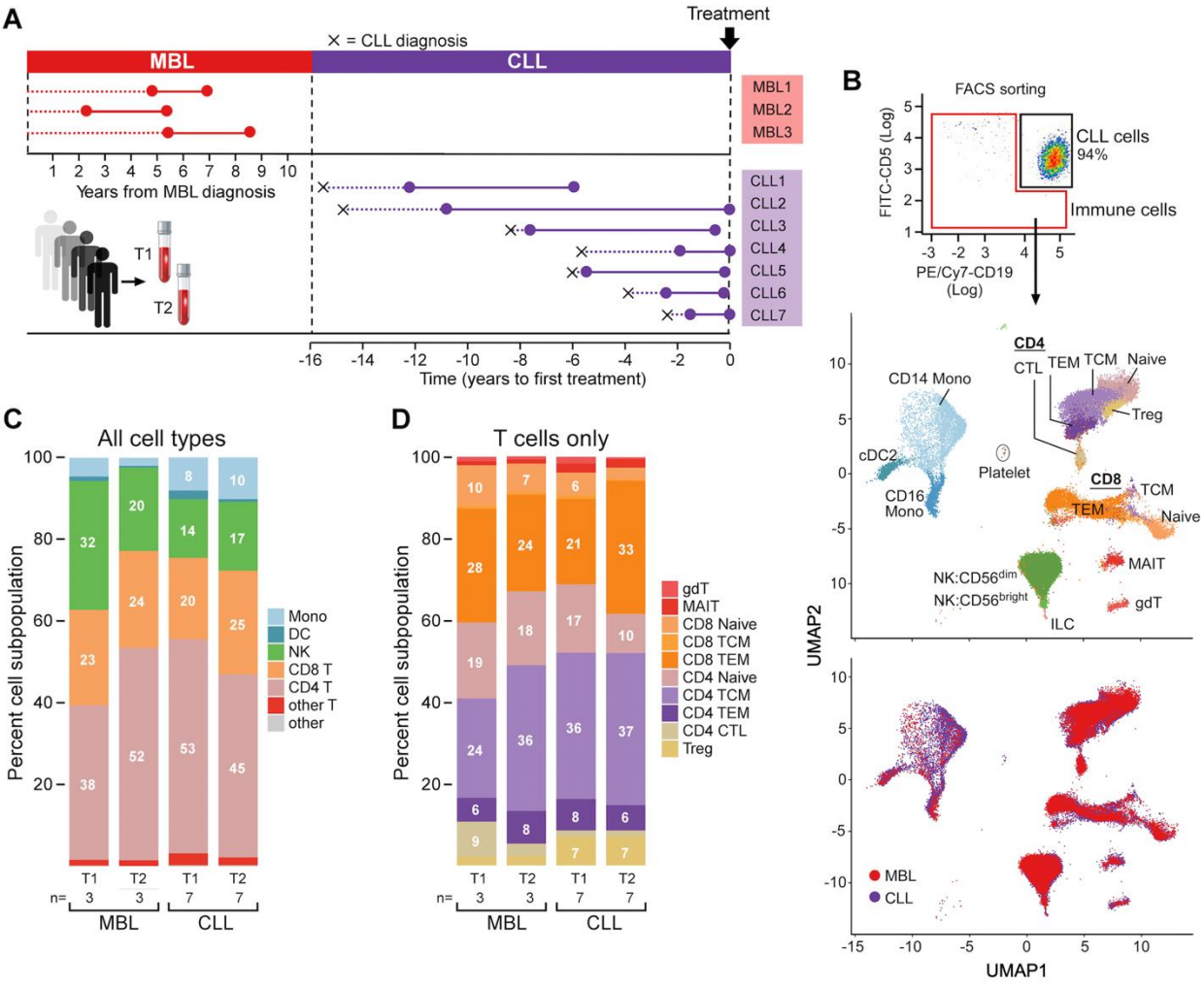
A
Treatment
× = CLL diagnosis
MBL
CLL
MBL1
MBL2
MBL3
CLL1
CLL2
CLL3
CLL4
CLL5
CLL6
CLL7
Years from MBL diagnosis
T1
T2
Time (years to first treatment)
B
FACS sorting
CLL cells
94%
Immune cells
FITC-CD5 (Log)
PE/Cy7-CD19
(Log)
CD14 Mono
CD4
CTL
TEM
TCM
Naive
Treg
cDC2
Platelet
CD8
TCM
TEM
Naive
CD16
Mono
NK:CD56dim
NK:CD56bright
MAIT
gdT
ILC
UMAP2
MBL
CLL
UMAP1
C
All cell types
Percent cell subpopulation
Mono
DC
NK
CD8 T
CD4 T
other T
other
n=
MBL
CLL
D
T cells only
gdT
MAIT
CD8 Naive
CD8 TCM
CD8 TEM
CD4 Naive
CD4 TCM
CD4 TEM
CD4 CTL
Treg

Figure 2

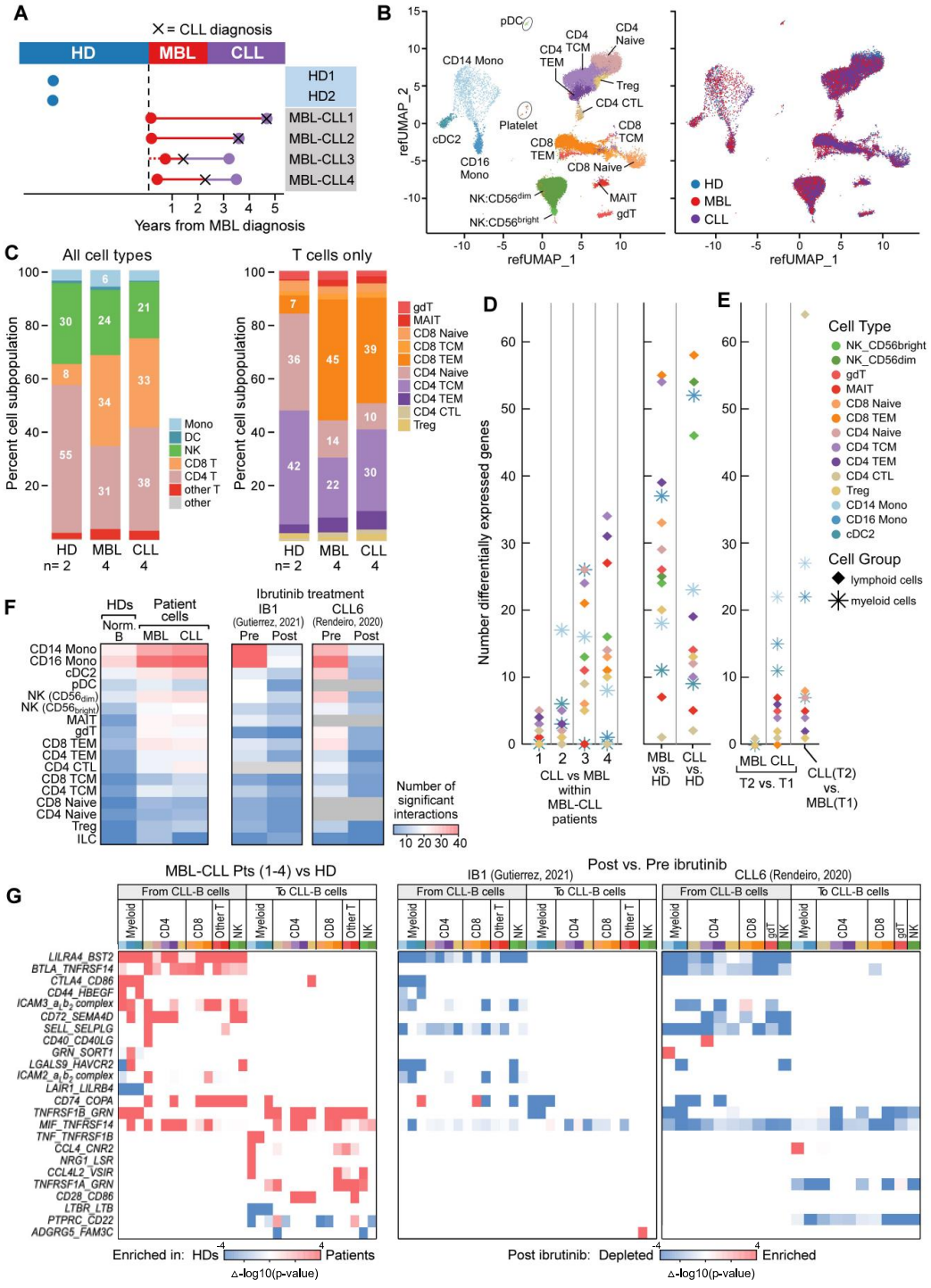
A
× = CLL diagnosis
HD
MBL
CLL
HD1
HD2
MBL-CLL1
MBL-CLL2
MBL-CLL3
MBL-CLL4
Years from MBL diagnosis
B
pDC
CD4 Naive
CD4 TCM
CD4 TEM
CD14 Mono
Treg
CD4 CTL
Platelet
CD8 TCM
cDC2
CD8 TEM
CD8 Naive
CD16 Mono
NK:CD56dim
MAIT
NK:CD56bright
gdT
refUMAP_1
refUMAP_2
HD
MBL
CLL
C
All cell types
T cells only
Percent cell subpopulation
Mono
DC
NK
CD8 T
CD4 T
other T
other
gdT
MAIT
CD8 Naive
CD8 TCM
CD8 TEM
CD4 Naive
CD4 TCM
CD4 TEM
CD4 CTL
Treg
HD n= 2
MBL 4
CLL 4
D
Number differentially expressed genes
CLL vs MBL within MBL-CLL patients
MBL vs. HD
CLL vs. HD
E
Cell Type
NK_CD56bright
NK_CD56dim
gdT
MAIT
CD8 Naive
CD8 TEM
CD4 Naive
CD4 TCM
CD4 TEM
CD4 CTL
Treg
CD14 Mono
CD16 Mono
cDC2
Cell Group
lymphoid cells
myeloid cells
MBL CLL
T2 vs. T1
CLL(T2) vs. MBL(T1)
F
HDs
Patient cells
Norm. B
MBL
CLL
Ibrutinib treatment
IB1 (Gutierrez, 2021)
CLL6 (Rendeiro, 2020)
Pre
Post
CD14 Mono
CD16 Mono
cDC2
pDC
NK (CD56dim)
NK (CD56bright)
MAIT
gdT
CD8 TEM
CD4 TEM
CD4 CTL
CD8 TCM
CD4 TCM
CD8 Naive
CD4 Naive
Treg
ILC
Number of significant interactions
10 20 30 40
G
MBL-CLL Pts (1-4) vs HD
Post vs. Pre ibrutinib
IB1 (Gutierrez, 2021)
CLL6 (Rendeiro, 2020)
From CLL-B cells
To CLL-B cells
Myeloid
CD4
CD8
Other T
gdT
NK
LILRA4_BST2
BTLA_TNFRSF14
CTLA4_CD86
CD44_HBEGF
ICAM3_a1b2 complex
CD72_SEMA4D
SELL_SELPLG
CD40_CD40LG
GRN_SORT1
LGALS9_HAVCR2
ICAM2_a1b2 complex
LAIR1_LILRB4
CD74_COPA
TNFRSF1B_GRN
MIF_TNFRSF14
TNF_TNFRSF1B
CCL4_CNR2
NRG1_LSR
CCL4L2_VSIR
TNFRSF1A_GRN
CD28_CD86
LTBR_LTB
PTPRC_CD22
ADGRG5_FAM3C
Enriched in: HDs
Patients
Δ-log10(p-value)
Post ibrutinib: Depleted
Enriched

289